Applied Physics Express **00**, 000000 (2019) **LETTER**
https://doi.org/10.7567/1882-0786/aafa0d

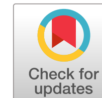

Ideal half-filled intermediate band position in $CuGaS_2$ generated by Sb-related defect complex: a first-principles study

Dan Huang[1,2], Yang Xue[1], Wentong Zhou[1], Jingwen Jiang[1], Hua Ning[1,2], Jin Guo[1,2], Yu-Jun Zhao[3*], Rongzhen Chen[4], and Clas Persson[5*]

[1]Guangxi Key Laboratory for Relativistic Astrophysics, Guangxi Colleges and Universities Key Laboratory of Novel Energy Materials and Related Technology, Guangxi Novel Battery Materials Research Center of Engineering Technology, Guangxi Key Laboratory of Processing for Non-Ferrous Metallic and Featured Materials, School of Physical Science and Technology, Guangxi University, Nanning 530004, People's Republic of China
[2]Guangxi Collaborative Innovation Center of Structure and Property for New Energy and Material, School of Material Science and Engineering, Guilin University of Electronic Technology, Guilin 541004, People's Republic of China
[3]Department of Physics and Key Laboratory of Advanced Energy Storage Materials of Guangdong Province, South China University of Technology, Guangzhou 510640, People's Republic of China
[4]Department of Computer Science and Engineering, Chalmers University of Technology, SE-41296 Gothenburg, Sweden
[5]Department of Physics and Centre for Materials Science and Nanotechnology, University of Oslo, P.O. Box 1048 Blindern, NO-0316 Oslo, Norway

*E-mail: zhaoyj@scut.edu.cn(Y.J.Z.); clas.persson@fys.uio.no(C.P.)

Received December 6, 2018; accepted December 19, 2018; published online MM DD, 2019

Cu-based chalcopyrite compounds have attracted much attention for photovoltaic application, while some of them (like $CuGaS_2$) have energy gaps greater than the optimal value. An isolated and half-filled intermediate band located at the lower part of its original band gap exhibits in $CuGaS_2$ with ($Sb_{Ga} + Zn_{Ga}$) or ($Sb_{Ga} + V_{Cu}$) defect complex, in line with the intrinsic p-type conductivity of the host, revealed from our first-principles calculations. Subsequently, the absorption coefficients of $CuGaS_2$ can cover the full solar light spectrum efficiently. Based on the defect formation energy calculations, however, these defect complexes are hard to reach a large concentration under equilibrium condition. Nevertheless, non-equilibrium growth methods are suggested to prepare samples inheriting the excellent adsorption coefficients.
© 2019 The Japan Society of Applied Physics

As a feasible way to solve the energy crisis in the future, solar energy and solar cell have captured much attentions[1,2] in recent years. The efficiency records in the laboratory of the solar cells based on Cu(In, Ga)Se_2 and $Cu_2ZnSn(S,Se)_4$ have reached 22.6%[3] and 12.6%,[4] respectively. Beside the Cu-based semiconductors, organic-inorganic hybrid pervoskite compounds like $CH_3NH_3PbI_3$ have achieved a rapid progress over the past decade.[5] However, the photovoltaic efficiency of the compounds with a single band gap is restricted in 31.0%[6] under solar illumination at one sun concentration from the so-called "Shockley and Queisser limit,"[6] which hinders the development space of the thin-film solar cells.

In 1997, Ref. 7 proposed a concept of intermediate band solar cell (IBSC), which fulfills three-photons absorption through an half-filled intermediate band (IB) inserted in the main band gap of the host. The theoretical efficiency of IBSC increases remarkably to 46.8% and 63.2%[8] at one sun and full concentration, respectively. The corresponding optimal band gaps of the host for IBSC are 2.40 and 1.93 eV.[7,9] Owing to the ideal width of band gap and the success of Cu (In, Ga)Se_2 in thin-film solar cell, $CuGaS_2$ among the chalcopyrite compounds has attracted the most attentions as the host for IBSC both from experimental and theoretical researchers. From the aspect of experiments, different groups have observed the sub-gap absorptions associated with IB in Ti,[10] Cr,[11] Fe[12] and Sn[13] doped $CuGaS_2$ samples. From the earlier first-principles studies[14,15] based on LDA/GGA functional, the half-filled IB and the consequent absorption coefficient related to sub-band gaps has been reported in transition metals[14] (i.e. Ti and Cr) and group-IV elements[15] (i.e. C, Si, Ge, and Sn) doped at Ga site in $CuGaS_2$. Recently, due to the more accurate results on the width of band gap and position of IB than those from the traditional LDA or GGA functional, the advanced hybrid functional like HSE (i.e. Heyd, Scuseria, and Ernzerhof) was adopted to study $CuGaS_2$ doping with Ti,[16] Fe,[17,18] Co[18] and Sn[13] as the absorber for IBSC. A lower filled and a higher empty sub-bands have been reported in Ti doped $CuGaS_2$,[16] meanwhile an unfilled IB was also discovered in Co and Fe doped $CuGaS_2$.[17,18] These new results should be origin from the accurate description on crystal field splitting and localized characteristic of d-orbital after the adoption of HSE functional. A half-filled IB still existed in the main band gap in Sn-doped $CuGaS_2$, however, the position of IB and the calculated Fermi energy level are located at upper part of the main band gap,[13] which implies that the sample should have an n-type semiconducting conductivity. Owing to the high valence band positions of these Cu-based chalcopyrite compounds,[19,20] the intrinsic p-type defect like Cu vacancy is easily formed and then makes them as intrinsic p-type semiconductors.[21] The contradictory between the position of half-filled IB and the intrinsic p-type may result in electron transfer, n-type and p-type defects combination etc. and then destroy the half-filled property or even the presence of IB. Therefore, to keep the position of the half-filled IB consistent with the intrinsic p-type property of the host, it is better to find an IB located in the lower part of the main band gap in $CuGaS_2$.

In this letter, a half-filled IB is found in $CuGaS_2$ with ($Sb_{Ga} + Zn_{Ga}$) or ($Sb_{Ga} + V_{Cu}$) defect complex, respectively. Especially, the half-filled IB and the calculated Fermi energy level are located at the lower part of the original band gap of $CuGaS_2$ host, which is in line with the intrinsic p-type semiconducting of $CuGaS_2$. The absorption coefficient of $CuGaS_2$ with ($Sb_{Ga} + Zn_{Ga}$) or ($Sb_{Ga} + V_{Cu}$) is significantly enhanced from 1.0 to 2.5 eV in the solar light spectrum owing to the presence of IB. The formation energies of related point defects and defect complexes under equilibrium condition are evaluated. The defect formation energies of these defect complexes are unfortunately still large, even under the most suitable chemical growth condition.

© 2019 The Japan Society of Applied Physics

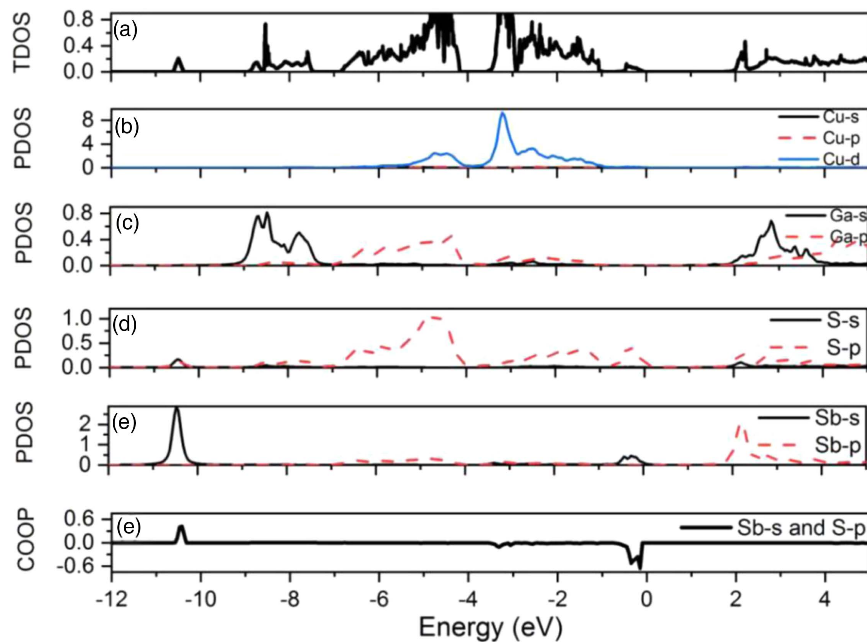

Fig. 1. (Color online) The total density of states (TDOS), partial density of states (PDOS) of Cu, Ga, S and Sb, and COOP between Sb-s and S-p state in Sb doped $CuGaS_2$.

Therefore, the non-equilibrium growth method with deliberate controlling is needed to prepare the proposed samples.

Our first-principles calculations are carried out by the VASP package based on density functional theory.[22] The projector augmented-wave method is used to describe the interactions between the valence electrons and the core. The hybrid exchange-correlation functional is chosen as the type developed by HSE.[23] In order to make the calculated band gap to meet the experimental value, the amount of Hartree–Fock exchange is adjusted to $\alpha = 0.30$ and the screening parameter $\omega = 0.20\ \text{bohr}^{-1}$ is kept. Our calculated lattice constants and the anion displacement parameter of $CuGaS_2$ are $a = 5.375$ Å, $c = 10.544$ Å and $u = 0.255$, which is in line with the experimental results[24] $a = 5.347$ Å, $c = 10.474$ Å and $u = 0.254$. The cut-off energy for the plane wave basis is set to 500 eV for all calculations. The electronic structure and optical property are calculated based on $\sqrt{2} \times \sqrt{2} \times 1$ supercell containing around 32 atoms, in which the $4 \times 4 \times 3$ Γ-centered Monkhorst–Pack k-point meshes[25] are adopted. Here, for the optical property calculation, the intraband transition correction is conducted for the system containing half-filled IB by employing an empirical Drude term.[26] The defect formation energy are calculated by using $2 \times 2 \times 1$ supercell containing around 64 atoms, in which the $2 \times 2 \times 2$ Γ-centered Monkhorst–Pack k-point meshes are utilized.

Figure 1 presents the total density of states (TDOS), partial density of states (PDOS) of Cu, Ga, S and Sb, and COOP (i.e. crystal orbital overlap populations[27]) between Sb-s and S-p state in $CuGaS_2$ with Sb_{Ga}. In consistent with former studies,[20,28] the original valence band maximum (VBM) and conduction band minimum in $CuGaS_2$ come from the antibonding states between Cu-d and S-p states and that between Ga-s and S-s,p states, respectively. After Sb doping at Ga site, a new fully-filled peak appears above the original VBM, which is corresponding to the lone-pair s states of Sb. The lone-pair s states are also reported from HSE-calculations[29] in $CuInSe_2$ with Sb_{In}. The lone-pair s electrons of Sb_{Ga} cannot be ionized and then Sb_{Ga} should serve as a neutral defect in $CuGaS_2$. From the PDOS of S and Sb, one can observe that the additional peak above the original VBM is composed of S-p state and Sb-s state. Making further analysis on COOP [Fig. 1(f)], one can understand that the new VBM origins from the antibonding state between Sb-s and S-p states.

Figure 2(a) shows the band structure of pure $CuGaS_2$, indicating a direct gap semiconductor. Our calculated band gap is 2.42 eV, which is close to the experimental data 2.43 eV.[30] As shown in Fig. 2(b), an isolated and fully-filled IB is presented above the original VBM after Sb_{Ga} doping, corresponding to the additional peak above the original VBM in the figure of TDOS. The widths of the main band gap and the fully-filled IB are 2.42 eV and 0.84 eV, respectively. Since the isolated band is fully occupied, another p-type intrinsic defect Cu vacancy (V_{Cu}) or extrinsic defect Zn substituting at Ga (Zn_{Ga}) is introduced in Sb-doped $CuGaS_2$ to produce a half-filled IB. The V_{Cu} or Zn_{Ga} is put next to Sb_{Ga} in the supercell with defect complex ($V_{Cu} + Sb_{Ga}$) or ($Zn_{Ga} + Sb_{Ga}$). Since V_{Cu} and Zn_{Ga} are one valence acceptors, the fully-filled IBs become half-occupied and move upwards as presented in Figs. 2(c) and 2(d). The isolated and half-filled IBs appear in the lower part of the original band gaps in $CuGaS_2$ with defect complex ($V_{Cu} + Sb_{Ga}$) or ($Zn_{Ga} + Sb_{Ga}$). Then, the position of half-filled IB and calculated Fermi energy level are consistent with the intrinsic p-type conductivity of $CuGaS_2$, which can avoid the transfer of the electron on IB and then increase the stability of the half-filled IB. The widths of the main band gap and the half-filled IB are 2.73 and 0.94 eV for ($V_{Cu} + Sb_{Ga}$) and 2.49 and 0.95 eV for ($Zn_{Ga} + Sb_{Ga}$).

From the absorption coefficients in Fig. 3, one can observe that pure $CuGaS_2$ cannot absorb the visible light effectively owing to its wide band gap. After Sb-doping, the absorption coefficient has a red shift due to the presence of the isolated

© 2019 The Japan Society of Applied Physics

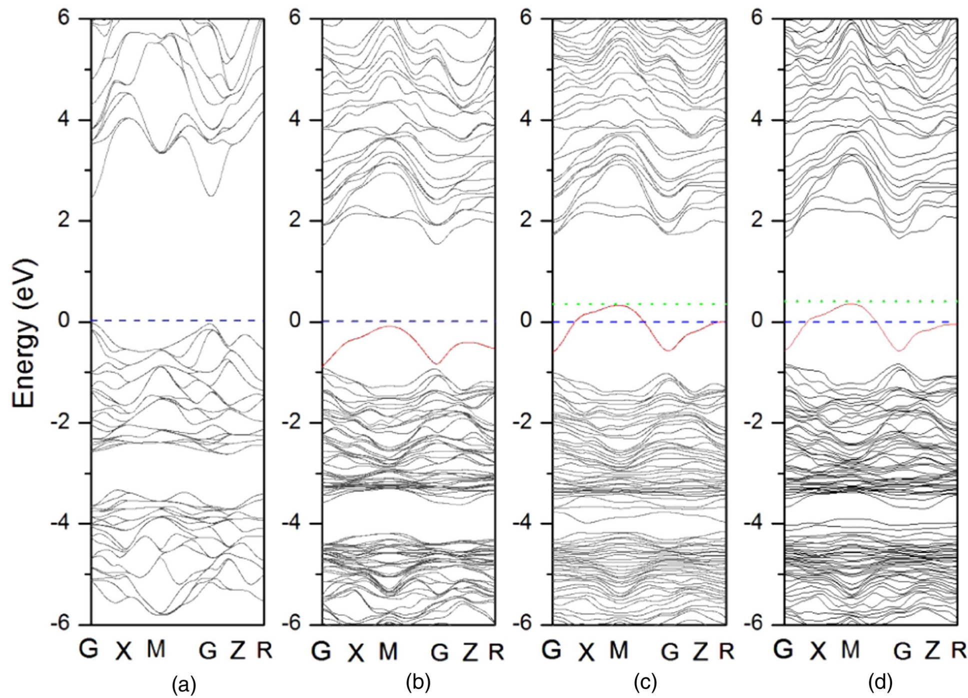

Fig. 2. (Color online) The calculated band structure of pure $CuGaS_2$ (a), $CuGaS_2$ with Sb_{Ga} defect (b), $CuGaS_2$ with ($Sb_{Ga} + V_{Cu}$) (c) and ($Sb_{Ga} + Zn_{Ga}$) (d) defect complexes. The red lines indicate the new bands after doping. The dotted green lines stand for the middle of the band gap without considering the half-filled intermediate bands. The Fermi energy levels in each system are set as zero, which are indicated as the dashed blue line.

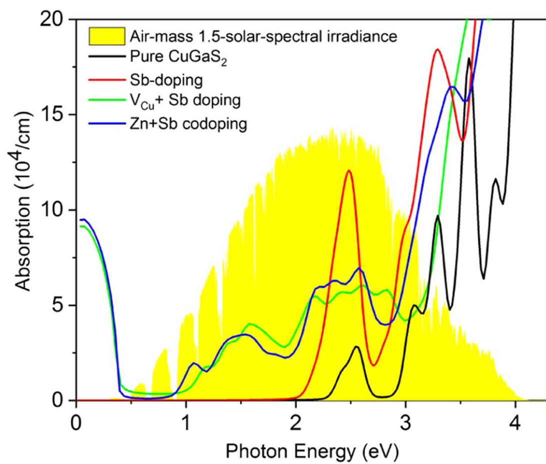

Fig. 3. (Color online) The absorption coefficients of pure $CuGaS_2$ and $CuGaS_2$ with Sb_{Ga} defect, ($Sb_{Ga} + V_{Cu}$) and ($Sb_{Ga} + Zn_{Ga}$) defect complexes. The Air-mass 1.5-solar-sepctral irradiance is shown as a reference.

and fully-filled band above the original VBM. When the half-filled IB is inserted in the main band gap of $CuGaS_2$, the three-photon absorption can be realized and the absorption coefficients can cover the solar light spectrum effectively in $CuGaS_2$ with defect complexes as shown in Fig. 3. Compared with the absorption coefficients before intraband correction, the revised absorption coefficients have new absorption peaks from 0 to 0.4 eV owing to the intraband absorption in the half-filled IB. Since the electronic structures and optical properties are calculated based on the supercell with a large concentration of defect complexes, the real samples need to contain a large amount of defect complex ($Sb_{Ga} + V_{Cu}$) or ($Sb_{Ga} + Zn_{Ga}$) to be used as the absorber for IBSC.

In order to evaluate the possibility of the formation of defect complexes, we have calculated the formation energies of related defects and defect complexes according to:[31]

$$\Delta E(D^0) = E(D^0) - E(0) + \sum_{\alpha} n_\alpha(\Delta\mu_\alpha + \mu_\alpha^{\mathrm{solid}}), \quad (1)$$

where $E(D^0)$ and $E(0)$ are the calculated energies from the supercells with and without defects $\mu_\alpha^{\mathrm{solid}}$ is the chemical potential of elementary solid and $\Delta\mu_\alpha$ is chemical potential of each element relative to $\mu_\alpha^{\mathrm{solid}}$. n_α is the number of atoms involving the defects or defect complexes formation. If an atom is shifted in the supercell, n_α is equal to -1, while n_α is equal to $+1$ if an atom is moved out the supercell.

Under the specific equilibrium growth conditions, the relative chemical potentials of each element $\Delta\mu_\alpha$ can be changed within a certain range. Their summation should be equal to the formation enthalpy of $CuGaS_2$ to keep the stability of the host:

$$\Delta\mu_{\mathrm{Cu}} + \Delta\mu_{\mathrm{Ga}} + 2\Delta\mu_{\mathrm{S}} = \Delta H(\mathrm{CuGaS_2}) = -2.98\ \mathrm{eV}. \quad (2)$$

To avoid the precipitation of elemental solids and other competing compounds, the allowed ranges of $\Delta\mu_\alpha$ are further restricted within the shaded area in Fig. 4(a). Within this area, six points (i.e. A, B, C, D, E and F) on the boundary, which are corresponding to different extreme growth conditions, are chosen for the calculations of defect formation energies. The detailed values of the relative chemical potentials of Cu, Ga and S under the six growth conditions are shown in Fig. 4(a). The maximum allowed values of the chemical potentials for Sb and Zn are adopted for the defect formation calculations, which are limited by the precipitation of Sb_2S_3 and ZnS.

Figure 4(b) shows the defect formation energies of related point defects Sb_{Ga}, Sb_S, Zn_{Ga} and V_{Cu}. The results show that Sb can occupy Ga site or S site depending on the chemical potentials, which are corresponding to different sample growth conditions. Under Ga-rich, Cu-rich and S-poor condition (i.e. point A), Sb substituting S has the lowest formation energy. Under Ga-poor and S-rich conditions

 © 2019 The Japan Society of Applied Physics

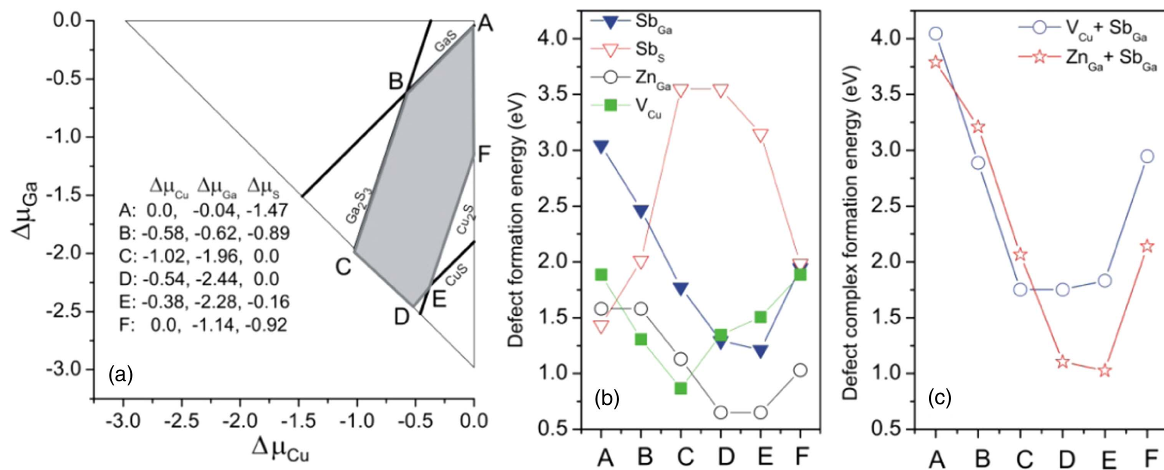

Fig. 4. (Color online) The allowed chemical potentials (a) of $\Delta\mu_{Cu}$, $\Delta\mu_{Ga}$ and $\Delta\mu_S$ in $CuGaS_2$. Six representative points (i.e. A, B, C, D, E and F) have been selected to estimate the defect formation energy. The defect formation energies of defects (b) and defect complexes (c) under different conditions.

(i.e. points D and E), Sb substituting Ga has the lowest formation energy. Coincidently, Zn substituting Ga also has the lowest formation energy under D and E points. Meanwhile, Cu vacancy has the lowest formation energy under Cu-poor and S-rich condition (i.e. point C). The p-type defects V_{Cu} and Zn_{Ga} have low formation energies under certain conditions, which is consistent with the p-type of $CuGaS_2$ from experiments.[21,32] Owing to the electron transfer between Sb_{Ga} and Zn_{Ga} (or Sb_{Ga} and V_{Cu}), the two point defects can attract with each other and then bind in a close configuration. Our calculated binding energies for ($Sb_{Ga} + V_{Cu}$) and ($Sb_{Ga} + Zn_{Ga}$) are 0.89 and 0.84 eV, respectively. The lowest formation energies for defect complexes ($Sb_{Ga} + Zn_{Ga}$) and ($Sb_{Ga} + V_{Cu}$) are 1.03 and 1.75 eV [see Fig. 4(c)], respectively. Based on the Boltzmann distribution law and adopted 1000 K as the sample growth temperature, we can get the concentrations of ($Sb_{Ga} + Zn_{Ga}$) and ($Sb_{Ga} + V_{Cu}$) defect complexes are 4.7×10^{-16} and $2.3 \times 10^{-12}\,cm^{-3}$, which are far away from the adopted concentrations in our calculations. Therefore, the non-equilibrium growth method are needed to generate a large concentration of defect complex and then form the IB other than defect levels in the main band gap. Moreover, the desired ratio and the configuration between the single point defects are also needed to deliberately control during the non-equilibrium growth.[33]

In conclusion, based on the HSE hybrid functional calculations, the IB located at the lower part of the original band gap has been found in the p-type semiconductor $CuGaS_2$ with ($Sb_{Ga} + Zn_{Ga}$) or ($Sb_{Ga} + V_{Cu}$) defect complex. This feature can maintain the stability of the electrons on IB. Owing to the insertion of the half-filled IB, the absorption coefficients can cover the solar light spectrum efficiently with the presence of defect complexes. $CuGaS_2$ with ($Sb_{Ga} + Zn_{Ga}$) or ($Sb_{Ga} + V_{Cu}$) defect complex has the ideal electronic structure as the absorber for IBSC. However, the formation energies of these defect complexes under the equilibrium condition are too large to achieve a high concentration. Therefore, the non-equilibrium growth method with deliberate controlling is needed to prepare our proposed samples.

Acknowledgments This work was financially supported by the National Natural Science Foundation of China (Grant Nos. 61664003, 11574088 and 51571065), Hundred-Talent Program in Guangxi Province, Innovation-Driven Development Foundation of Guangxi Province (Grant No. AA17204063), and the Research Council of Norway (project: 243642). We acknowledge the Swedish National Infrastructure for Computing for providing access to supercomputer resources.

1) A. Polman, M. Knight, E. C. Garnett, B. Ehrler, and W. C. Sinke, Science **352**, aad4424 (2016).
2) N. S. Lewis, Science **351**, aad1920 (2016).
3) P. Jackson, R. Wuerz, D. Hariskos, E. Lotter, W. Witte, and M. Powalla, Phys. Status Solidi-Rapid Res. Lett. **10**, 583 (2016).
4) W. Wang, M. T. Winkler, O. Gunawan, T. Gokmen, T. K. Todorov, Y. Zhu, and D. B. Mitzi, Adv. Energy Mater. **4**, 1301465 (2014).
5) L. Etgar, P. Gao, Z. Xue, Q. Peng, A. K. Chandiran, B. Liu, M. K. Nazeeruddin, and M. Grätzel, J. Am. Chem. Soc. **134**, 17396 (2012).
6) W. Shockley and H. J. Queisser, J. Appl. Phys. **32**, 510 (1961).
7) A. Luque and A. Martí, Phys. Rev. Lett. **78**, 5014 (1997).
8) A. S. Brown and M. A. Green, J. Appl. Phys. **92**, 1329 (2002).
9) A. Luque and A. Marti, Adv. Mater. **22**, 160 (2010).
10) X. Lv, S. Yang, M. Li, H. Li, J. Yi, M. Wang, G. Niu, and J. Zhong, Sol. Energy **103**, 480 (2014).
11) P. Chen, M. Qin, H. Chen, C. Yang, Y. Wang, and F. Huang, Phys. Status Solidi. A **210**, 1098 (2013).
12) B. Marsen, S. Klemz, T. Unold, and H. W. Schock, Prog. Photovolt. **20**, 625 (2012).
13) C. Yang, M. Qin, Y. Wang, D. Wan, F. Huang, and J. Lin, Sci. Rep. **3**, 1286 (2013).
14) I. Aguilera, P. Palacios, and P. Wahnón, Sol. Energy Mater. Sol. Cells **94**, 1903 (2010).
15) C. Tablero, Thin Solid Films **519**, 1435 (2010).
16) J. Hashemi, A. Akbari, S. Huotari, and M. Hakala, Phys. Rev. B **90**, 075154 (2014).
17) J. Koskelo, J. Hashemi, S. Huotari, and M. Hakala, Phys. Rev. B **93**, 165204 (2016).
18) M. Han, X. Zhang, and Z. Zeng, RSC Adv. **4**, 62380 (2014).
19) S. B. Zhang, S. H. Wei, and A. Zunger, Phys. Rev. Lett. **84**, 1232 (2000).
20) S. Chen, X. G. Gong, and S. H. Wei, Phys. Rev. B **75**, 205209 (2007).
21) W. J. Jeong and G. C. Park, Sol. Energy Mater. Sol. Cells **75**, 93 (2003).
22) G. Kresse and J. Hafner, Phys. Rev. B **47**, 558 (1993).
23) M. J. Lucero, T. M. Henderson, and G. E. Scuseria, J. Phys.: Condens. Matter **24**, 145504 (2012).
24) S. C. Abrahams and J. L. Bernstein, J. Chem. Phys. **59**, 5415 (1973).
25) H. J. Monkhorst and J. D. Pack, Phys. Rev. B **13**, 5188 (1976).
26) C. Ambrosch-Draxl and J. O. Sofo, Comput. Phys. Commun. **175**, 1 (2006).
27) S. Maintz, V. L. Deringer, A. L. Tchougréeff, and R. Dronskowski, J. Comput. Chem. **34**, 255 (2013).
28) Y. Zhang, L. Xi, Y. Wang, J. Zhang, P. Zhang, and W. Zhang, Comput. Mater. Sci. **108**, 239 (2015).

© 2019 The Japan Society of Applied Physics

29) J. S. Park, J. H. Yang, K. Ramanathan, and S. H. Wei, Appl. Phys. Lett. **105**, 243901 (2014).
30) J. A. Hollingsworth, K. K. Banger, M. H.-C. Jin, J. D. Harris, J. E. Cowen, E. W. Bohannan, J. A. Switzer, W. E. Buhro, and A. F. Hepp, Thin Solid Films **431-432**, 63 (2003).
31) S. B. Zhang, S. H. Wei, and A. Zunger, Phys. Rev. B **63**, 075205 (2001).
32) S. F. Chichibu, T. Ohmori, N. Shibata, T. Koyama, and T. Onuma, Appl. Phys. Lett. **85**, 4403 (2004).
33) H. Zeng, G. Duan, Y. Li, S. Yang, X. Xu, and W. Cai, Adv. Funct. Mater. **20**, 561 (2010).

© 2019 The Japan Society of Applied Physics